Oncogene (2014), 1–13

www.nature.com/onc

ORIGINAL ARTICLE

PHF2 histone demethylase acts as a tumor suppressor in association with p53 in cancer

K-H Lee[1], J-W Park[1,2], H-S Sung[2], Y-J Choi[2], WH Kim[3], HS Lee[3], H-J Chung[2], H-W Shin[1], C-H Cho[1,2], T-Y Kim[4], S-H Li[2], H-D Youn[1,2], SJ Kim[1,2,5] and Y-S Chun[1,2,5]

Plant homeodomain finger 2 (PHF2) has a role in epigenetic regulation of gene expression by demethylating H3K9-Me2. Several genome-wide studies have demonstrated that the chromosomal region including the PHF2 gene is often deleted in some cancers including colorectal cancer, and this finding encouraged us to investigate the tumor suppressive role of PHF2. As p53 is a critical tumor suppressor in colon cancer, we tested the possibility that PHF2 is an epigenetic regulator of p53. PHF2 was associated with p53, and thereby, promoted p53-driven gene expression in cancer cells under genotoxic stress. PHF2 converted the chromatin that is favorable for transcription by demethylating the repressive H3K9-Me2 mark. In an HCT116 xenograft model, PHF2 was found to be required for the anticancer effects of oxaliplatin and doxorubicin. In PHF2-deficient xenografts, p53 expression was profoundly induced by both drugs, but its downstream product p21 was not, suggesting that p53 cannot be activated in the absence of PHF2. To find clinical evidence about the role of PHF2, we analyzed the expressions of PHF2, p53 and p21 in human colon cancer tissues and adjacent normal tissues from patients. PHF2 was downregulated in cancer tissues and PHF2 correlated with p21 in cancers expressing functional p53. Colon and stomach cancer tissue arrays showed a positive correlation between PHF2 and p21 expressions. Informatics analyses using the Oncomine database also supported our notion that PHF2 is downregulated in colon and stomach cancers. On the basis of these findings, we propose that PHF2 acts as a tumor suppressor in association with p53 in cancer development and ensures p53-mediated cell death in response to chemotherapy.

Oncogene advance online publication, 21 July 2014; doi:10.1038/onc.2014.219

INTRODUCTION

Cancer is caused by the accumulation of multiple genetic and epigenetic alterations, and this process has been particularly well established in colon cancer. In particular, p53 loss is regarded as the most critical event in the progression from colon adenoma to carcinoma.[1] About 50% of colon cancers have a deletion or loss-of-function mutation of the *TP53* gene, and numerous studies have demonstrated that malignant phenotypes and chemoresistance are attributable to p53 loss in cancer cells.[2] However, it should be noted that half of the colon cancers have functional p53. Nonetheless, the p53-positive colon cancer cells have malignant phenotypes with a lower level of p21, which is a representative target of p53. These discrepant findings suggest that p53 is functionally deregulated even in p53-expressing cancers. Indeed, p53 activity is known to be finely controlled by epigenetic regulators.[3] For example, it has been reported that histone acetyltransferases, such as CBP/p300, PCAF, GCN5 and TIP60, and histone methyltransferases, such as PRMT1 and CARM1, are recruited by p53, and thereby, facilitate the p53-driven transcription.[4–7] In contrast, KDM1, the histone lysine demethylase, which is overexpressed in gliomas, was recently shown to inhibit p53-driven transcription by demethylating H3K4-Me2.[8]

As observed in most malignancies, a family history of colon cancer is one of the strongest risk factors for colon cancer. About 30% of all colorectal cancers are believed to have a genetic basis. Notably, a whole genome scan study identified a new colorectal cancer predisposition locus, chromosome 9q22.2–31.2, by analyzing genetic linkage in 53 colorectal cancer kindreds.[9] Interestingly, most of this region overlaps the chromosome 9q22.23–22.33, which is deleted in breast cancer and squamous cell carcinoma.[10,11] These reports strongly suggest that tumor suppressor genes are located in the chromosomal region, but no causal gene has been identified so far. We sought to identify epigenetic regulators whose genes are included in the region, and found that the PHF2 gene was located on chromosome 9q22.31.

PHF2 is a member of the Jumonji C family and harbors a plant homeodomain (PHD) finger and a Jumonji C (JmjC) domain. PHF2 was originally considered as a candidate gene for hereditary sensory neuropathy type-I.[12] The *PHF2* gene is deleted or hypermethylated in its promoter region in breast cancer and its expression is downregulated in head and neck cancer.[10,11] These two reports suggest the potential function of PHF2 as a tumor suppressor, but its precise role during tumor development has not been established. In terms of molecular function, PHF2 was found to demethylate H3K9-Me2 (lysyl dimethylation), and subsequently participate in epigenetic regulation of transcription.[13] For example, it was demonstrated that PHF2 binds to the transcription factors HNF4, CEBPα and NF-κB, and subsequently aids the expression of genes driven by these factors.[14–16] Considering that H3K9 modification provides a universal mechanism of epigenetic

[1]Ischemic/Hypoxic Disease Institute, Seoul National University College of Medicine, Seoul, Republic of Korea; [2]Department of Biomedical Sciences, Seoul National University College of Medicine, Seoul, Republic of Korea; [3]Department of Pathology, Seoul National University College of Medicine, Seoul, Republic of Korea; [4]Department of Internal Medicine, Seoul National University College of Medicine, Seoul, Republic of Korea and [5]Department of Physiology, Seoul National University College of Medicine, Seoul, Republic of Korea. Correspondence: Professor Y-S Chun, Department of Physiology, Seoul National University College of Medicine, 103 Daehak-ro, Jongno-gu, Seoul 110-799, Republic of Korea.
E-mail: chunys@snu.ac.kr
Received 30 January 2014; revised 5 May 2014; accepted 15 June 2014

gene regulation, PHF2 is expected to be involved in diverse biological functions in addition to its known roles.

Considering that PHF2 is a positive epigenetic regulator and that the PHF2 gene is located in the chromosomal region associated with tumor suppression, we hypothesized that PHF2 acts as a coactivator of transcription factors with tumor suppressive function. Accordingly, in the present study, we explored the roles of PHF2 as an epigenetic regulator of p53, as a tumor suppressor in cancer, and as a factor determining tumor sensitivity to anticancer drugs.

RESULTS

PHF2 is associated with p53 in cancer cells

We tested the possibility that PHF2 is involved in the p53 signaling pathway. As protein interaction is the first step for epigenetic regulation, we first checked whether PHF2 is associated with p53. Among the three members (PHF2, PHF8 and KIAA1718) of the KDM7 histone demethylase family, only PHF2 was co-precipitated with p53 in p53+/+ HCT116 colon cancer cells (Figure 1a). Moreover, p53 induced by doxorubicin also interacted with PHF2, and this interaction was cross-checked by changing the antibodies used for immunoprecipitation (Figure 1b). We confirmed the p53-PHF2 interaction in HCT116 p53+/+ cells ectopically expressing HA-p53 and F/S-PHF2 (Figure 1c). We next sought to identify the binding domains of PHF2 and p53. Among the four fragments of PHF2, the C terminus bound to p53 (Figure 1d). On the other hand, p53 fragments lacking DBD (DNA-binding domain) failed to bind to PHF2 (Figure 1e). These results suggest that the C terminus of PHF2 interacts with DBD of p53. Furthermore, with respect to our finding that the JmjC demethylase domain of PHF2 does not bind to p53, it appears that p53 may not be directly demethylated by PHF2, but rather it recruits PHF2 to target genes.

PHF2 is required for the cytotoxic action of anticancer drugs in p53-positive cancer cells

To understand the role of PHF2 in p53-driven apoptosis, we established stable cell lines by selecting p53+/+ and p53−/− HCT116 cells harboring shRNA-expressing lentiviruses. The cell lines were treated with anticancer drugs, such as oxaliplatin, doxorubicin and 5-fluorouracil, to stimulate the p53 signaling pathway. All of the anticancer drugs used in this study increased the sub-G1 (apoptotic cells) population in sh-control cells, but caused a less significant increase in the sub-G1 population in sh-PHF2 expressing p53+/+ HCT116 cells (Figure 2a, left panel). The sub-G1 populations in p53−/− HCT116 cells treated with anticancer agents were much less than those of p53+/+ HCT116, and also not affected by sh-PHF2 expression (Figure 2a, right panel). To confirm the role of PHF2 in cell death, we analyzed the cell viability using MTT and found that the cytotoxic effects of

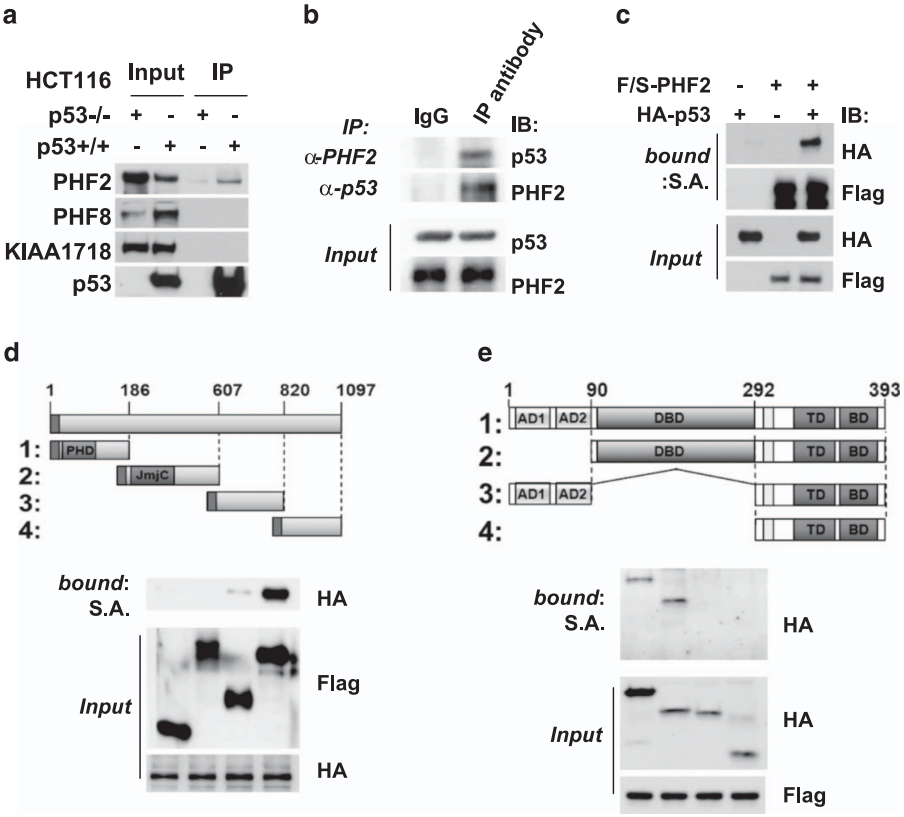

Figure 1. PHF2 directly bound to p53 in colon cancer cells. (**a**) p53+/+ and p53−/− HCT116 cells were treated with oxaliplatin for 16 h, and protein extracts were used for immunoprecipitation with p53 antibody. Immunoprecipitates were subjected to western blotting using α-PHF2, α-PHF8, α-KIAA1718 or α-p53 antibody. (**b**) p53+/+ HCT116 cells were treated with 0.5 μM doxorubicin for 8 h, immunoprecipitated with anti-PHF2 and immunoblotted using anti-p53 (upper panel). Co-immunoprecipitation was cross-checked by changing the antibodies used for immunoprecipitation and immunoblotting (second panel). (**c**) F/S-PHF2 and HA-p53 were ectopically expressed in p53+/+ HCT116 cells. Cell lysates were incubated with Streptavidin beads and bound proteins were eluted with biotin. Input and Streptavidin-bound proteins were detected by western blotting with indicated antibodies. (**d**) F/S-tagged PHF2 fragments[1–4] were co-expressed with HA-p53 plasmid in HEK293T cells. After F/S-PHF2 fragments were precipitated using Streptavidin beads, co-precipitated HA-p53 was detected by western blotting using anti-HA antibody. (**e**) HA-tagged p53 fragments were co-expressed with F/S-PHF2 in HEK293T cells. After F/S-PHF2 was precipitated using Streptavidin beads, co-precipitated HA-p53 proteins were detected by western blotting with anti-HA antibody.

these three anticancer drugs were attenuated by PHF2 knockdown (Figure 2b, upper panels). However, PHF2 knockdown did not increase cell viability in the p53 − / − HCT116 cells (Figure 2b, lower panels). Furthermore, pro-apoptotic enzymes were less activated by anticancer drugs in sh-PHF2 p53+/+ HCT116 cells than in sh-control cells (Figure 2c, left panel). Apoptotic markers were not induced by anticancer agents in the HCT116 p53 − / − cells (Figure 2c, right panel). To examine the role of PHF2 in p53 activation in cancers other than colon cancer, we stably expressed sh-PHF2 in cell lines expressing functional p53 (HepG2, MKN-74 and MCF7) and in cell lines lacking functional p53 (Hep3B, KATO III and MDA-MB231). Consequently, PHF2 knockdown induced cellular resistances to anticancer agents in p53-positive cell lines, but not in p53-negative cell lines (Figure 2d). These results further support our notion that PHF2 participates in p53-mediated apoptosis.

PHF2 has an essential role in the p53 signaling pathway

When the p53+/+ or p53 − / − HCT116 cells stably expressing sh-PHF2 were treated with doxorubicin, the expressions of p53 and its targets (p21, Hdm2 and Bax) were profoundly induced in sh-control/p53(+/+) cells, but not in sh-PHF2/p53(+/+) cells (Figure 3a). As expected, expressions of p21, Hdm2 and Bax were not induced by doxorubicin in p53-null cell lines, which confirms that these proteins are the specific targets of p53 in HCT116 cells. In addition, oxaliplatin and 5-fluorouracil also activated the p53

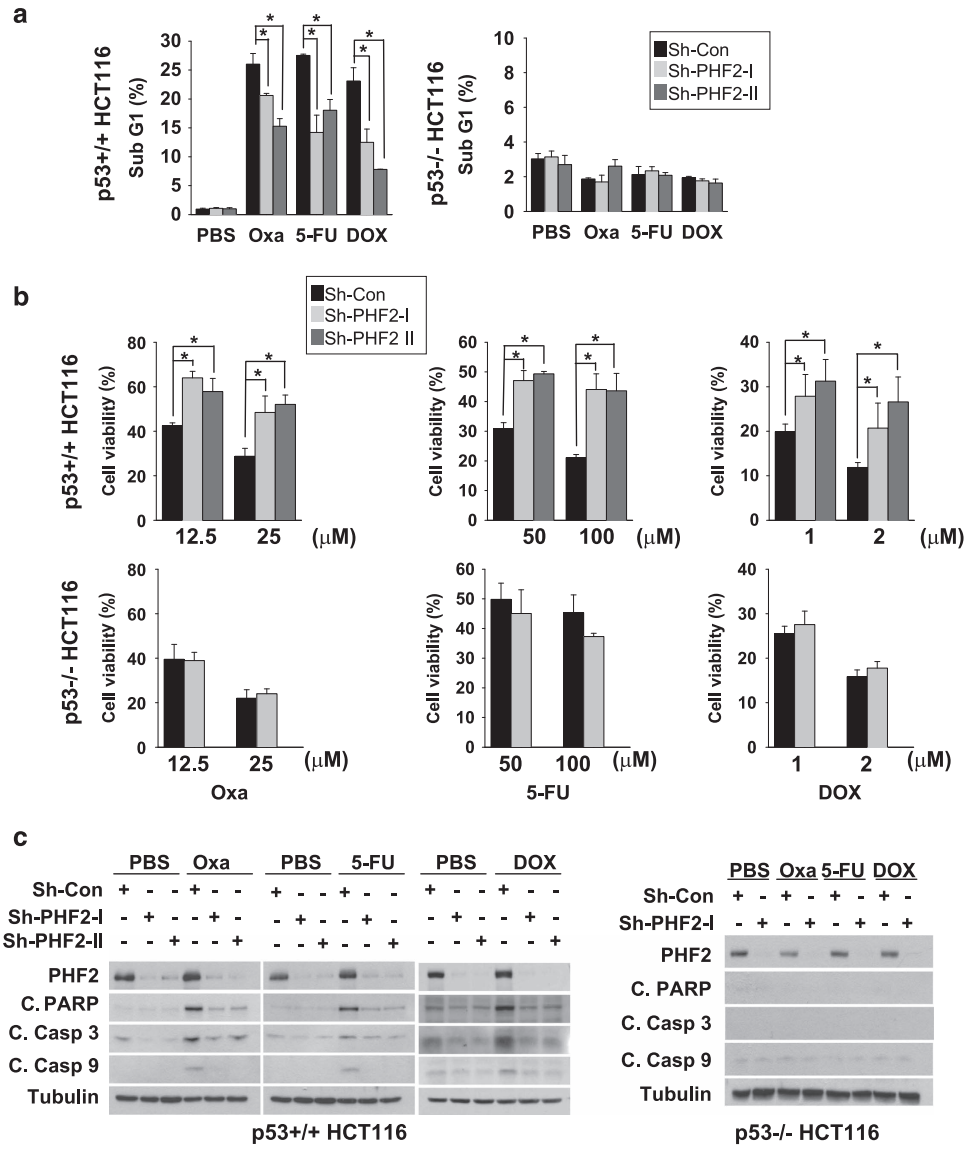

Figure 2. PHF2 promoted p53-dependent cell death induced by anticancer drugs in HCT116 cells. (**a**) Stable p53+/+ or p53 − / − HCT116 cells transfected with Sh-Con or Sh-PHF2 lentivirus were treated with the indicated anticancer drugs (25 μM of oxaliplatin, 100 μM of 5-FU and 2 μM of doxorubicin) for 2 days and then fixed for propidium iodide (PI) staining and cell cycle analysis. Cell populations in the sub-G1 phase were analyzed in more than three different experiments and the results are presented as means ± s.d. *$P < 0.05$ versus the Sh-Con group. (**b**) After treatment with the indicated anticancer drugs for 2 days, HCT116 stable cells were incubated with MTT solution to evaluate the cell viability. Bars represent the means ± s.d. of more than three independent experiments, and *$P < 0.05$ between two groups. (**c**) HCT116 stable cells were treated with phosphate-buffered saline, 12.5 μM oxaliplatin, 50 μM 5-FU or 0.5 μM doxorubicin for 16 h and apoptotic markers were analyzed by western blotting using indicated antibodies. (**d**) After being treated with the indicated anticancer drugs for 2 days, stable cells were incubated with MTT solution to evaluate the cell viability. Bars represent the means ± s.d. of more than three independent experiments, and *$P < 0.05$ between two groups.

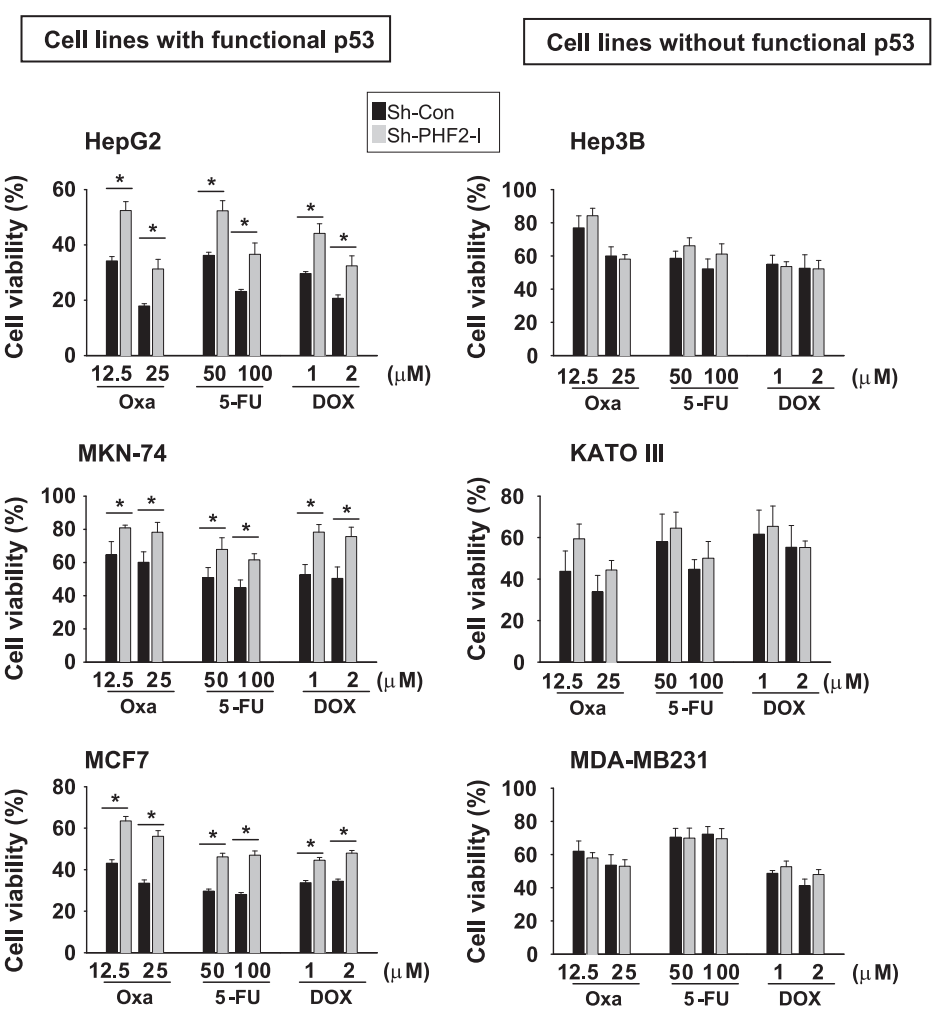

Figure 2. Continued.

signaling pathway, which was attenuated by PHF2 knockdown (Figure 3b). Furthermore, expressions of p21/*CDKN1A*, *BAX* and *HDM2* were induced at the transcriptional level by anticancer drugs, and their expressions were reduced by PHF2 knockdown (Figure 3c). The effect of PHF2 on p53 activation in cancers other than colon cancer was observed. We found that the inductions of p53 target genes by anticancer drugs were attenuated by PHF2 knockdown in p53-positive cell lines, but not in p53-negative cell lines (Figure 3d). These findings indicate that PHF2 is essential for p53-driven gene expression.

PHF2 demethylates methylated histone H3K9 at p53 target promoters

We next investigated the mechanism by which PHF2 regulates p53-driven transcription. As it was reported that PHF2 reverses H3K9 dimethylation, we tested the possibility that PHF2 is recruited by p53 and modifies chromatin towards active transcription. We checked histone methylation status in sh-control and sh-PHF2 stable cell lines and found that the dimethylated H3K9 level was elevated by PHF2 knockdown (Supplementary Figure 1). To examine the role of PHF2 as a coactivator of p53, we checked the binding of p53 and PHF2 to the promoters of the p53 target gene, *CDKN1A* (P1+P2) and *HDM2* (P1′+P2′), using the ChIP analysis in p53 +/+, p53 −/− HCT116 (Figure 4b) and HepG2 (Figure 4c) cells. We used upstream primers for non-p53 binding sequence of each gene (NS1/NS2 for *CDKN1A* gene, NS1′/NS2′ for *HDM2* gene) as negative controls (Figure 4a). As expected, p53 bound to *CDKN1A* and *HDM2* promoters, and its binding was augmented by doxorubicin treatment in p53+/+ HCT116 cells. Interestingly, p53 binding to target DNAs was reduced by PHF2 knockdown (Figure 4b, the 1st column in the left panel). Moreover, PHF2 was recruited to p53 target sites (Figure 4b, the 2nd column in the left panel). Then we examined whether PHF2 regulates the histone methylation status in p53 target sites. Consequently, the H3K9-Me2 level in p53 target sites was reduced by doxorubicin, which was recovered by PHF2 knockdown (Figure 4b, the 3rd column in the left panel). Given that H3K9 dimethylation is unfavorable for transcription, PHF2 knockdown is likely to repress p53-driven transcription by inducing H3K9 dimethylation. Significant PCR signals were not detected by NS1/NS2, NS1′/NS2′ and *GAPDH* primers, verifying the p53 target gene specificities of ChIP. On the contrary, the bindings of p53 and PHF2 to *CDKN1* and *HDM2* promoters were negligible in p53−/− HCT116 cells. (Figure 4b, right panel). We also observed the similar findings in HepG2 cells expressing p53 (Figure 4c). The role of PHF2 as an epigenetic coactivator of p53 is summarized in Figure 4d.

PHF2 determines the responses of colon cancer to anticancer drugs

We examined the role of PHF2 in p53-mediated apoptosis *in vivo*. We implanted HCT116 cells, which stably express sh-control or sh-PHF2 RNA, into nude mice and monitored the tumor growth.

Before performing this experiment, we expected that sh-PHF2 tumors having a lower p53 activity would grow faster than sh-control tumors. However, the tumor growth was not different between sh-PHF2 and sh-control tumors (Figures 5a and b). While the HCT116 cell line was established for a long time, they might be able to escape from the tumor suppressive action of the basal level of p53. For this reason, PHF2 knockdown may not further increase the growth of HCT116 xenografts. To reinforce the p53 action in HCT116 tumor cells, we injected p53-activating anticancer drugs into mice weekly. The growth of HCT116 tumors was retarded after the 2nd injection of oxaliplatin and it was almost completely arrested after the 3rd injection. Surprisingly, sh-PHF2 tumors kept growing even after the 3rd injection of oxaliplatin (Figure 5a and Supplementary Figure 2). A similar effect of PHF2 knockdown was also observed when mice were injected with doxorubicin (Figure 5b). These results suggest that PHF2 suppression desensitizes HCT116 tumors to oxaliplatin and doxorubicin. Immunohistochemical analyses showed that both oxaliplatin and doxorubicin substantially induced p21 and p53 expression in control tumors. In PHF2-deficient tumors, however, p21 expression was barely induced by both drugs whereas p53 was highly expressed (Figures 5c and d, top). The p21 and p53 levels are statistically analyzed in the bottom panels of Figures 5c and d. These results further support our notion that PHF2 positively regulates the p53-mediated apoptosis induced by anticancer drugs. Moreover, this implies that PHF2 could be a biomarker for predicting tumor sensitivity to anticancer drugs.

PHF2 downregulation is associated with the functional repression of p53 in human colon and stomach cancer

To examine whether PHF2 is involved in colon cancer development, we analyzed the p53, p21 and PHF2 levels in cancer tissues and adjacent normal tissues from 30 colon cancer patients (Figure 6a). As p53 expression was highly variable in tumors, there were no significant differences in p53 levels between tumors and normal tissues (Figure 6b, left). This unexpected finding may be due to the fact that inactively mutated p53 persists in tumors, and

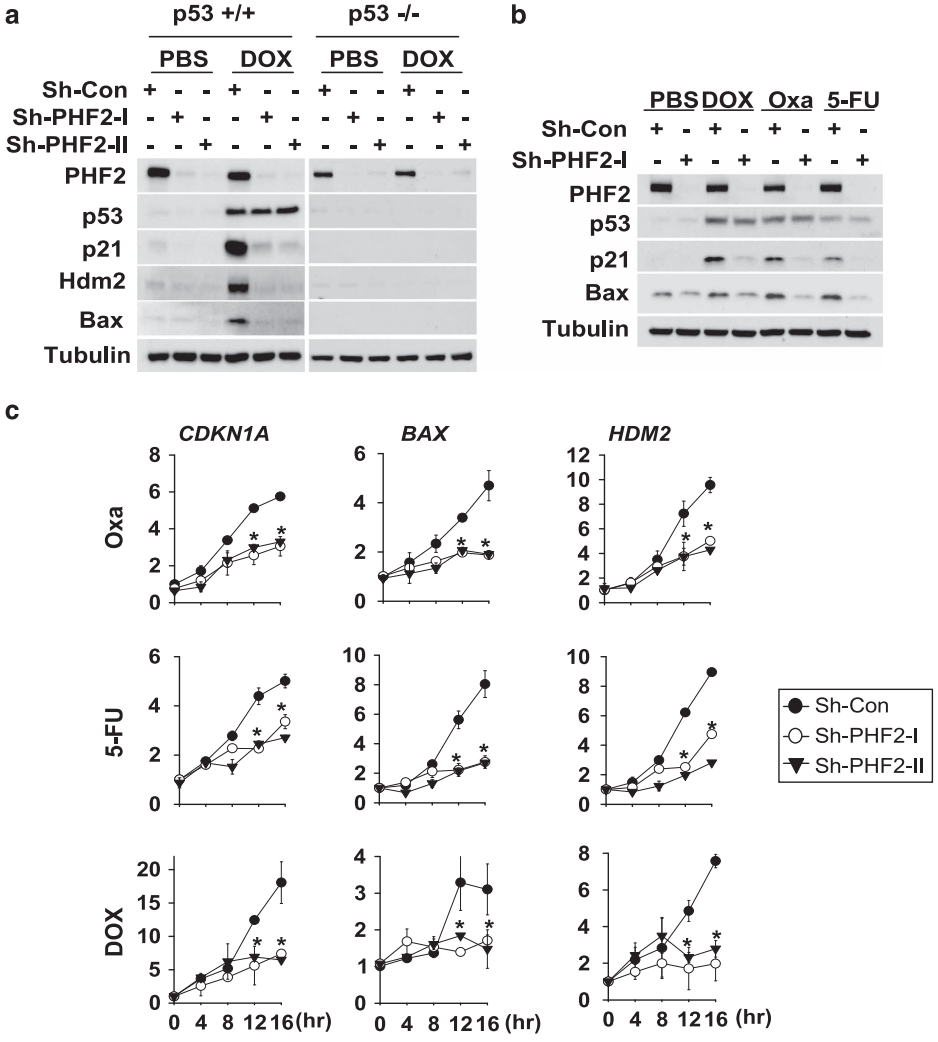

Figure 3. PHF2 played an essential role in the p53 signaling pathway. (**a**) p53+/+ or p53 − / − HCT116 cells were infected with Sh-Con or Sh-PHF2 lentivirus and then treated with 0.5 μM doxorubicin for 16 h. p53 and its downstream proteins were detected by western blotting. (**b**) Sh-Con or Sh-PHF2 stable HCT116 cells were treated with phosphate-buffered saline (PBS), 0.5 μM doxorubicin (DOX), 12.5 μM oxaliplatin (Oxa) or 50 μM 5′-fluorouracil (5-FU) for 16 h. Protein levels of PHF2, p53, p21 and Bax were determined by western blotting. (**c**) HCT116 stable cells were treated with the indicated drugs and then lysed at the indicated times. Relative mRNA levels of *CDKN1A*, *BAX* and *HDM2* were determined by RT–qPCR. Bars represents the means ± s.d. of three independent experiments, and $^*P < 0.01$ versus the Sh-Con group. (d) Sh-Con or Sh-PHF2 stable cell lines were treated with PBS, 0.5 μM doxorubicin (DOX), 12.5 μM oxaliplatin (Oxa) or 50 μM 5′-fluorouracil (5-FU) for 16 h. Protein levels of PHF2, p53, p21, Hdm2 and Bax were determined by western blotting.

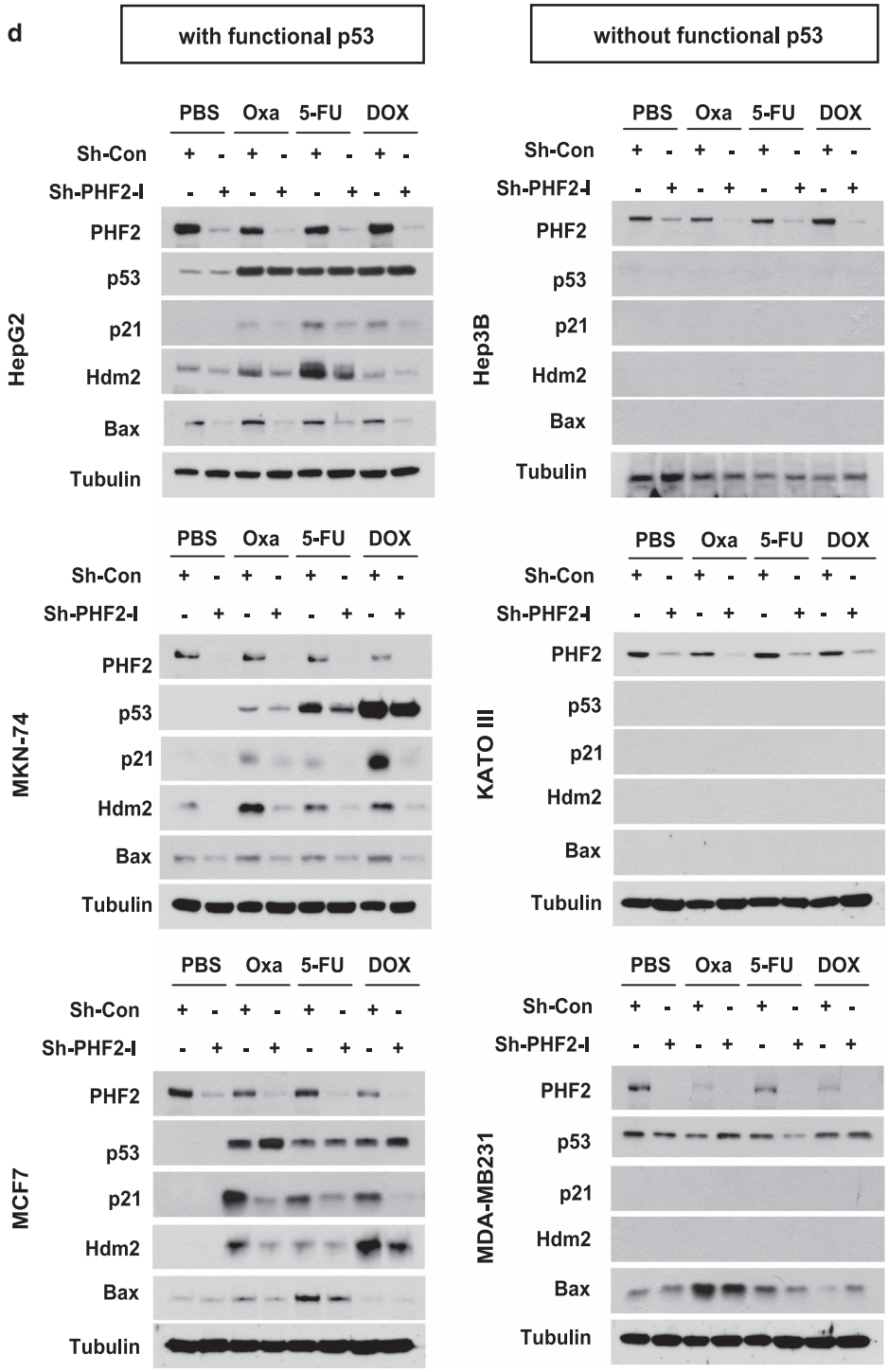

Figure 3. Continued.

therefore we checked the functionality of p53 by sequencing the entire region of p53 cDNA in each tumor. Consequently, 15 of 30 tumors had loss-of-function mutations of p53 whereas the other 15 tumors expressed wild-type p53 or functional p53 mutants (Supplementary Table 2). Accordingly, the p53 signaling pathway was expected to be functionally inhibited in 50% of colon cancers. As expected, p21 was downregulated in the tumors (Figure 6b, middle). Interestingly, PHF2 expression was also found to be reduced in tumors (Figure 6b, right). Reverese transcription–quantitaive PCR (RT–qPCR) analyses revealed that expressions of p21 and PHF2 in tumors were reduced at the transcriptional level (Figure 6c). To understand the mechanism by which the p21 expression is regulated in the tumors, we checked the relationship among p21, p53 and PHF2 in tumors. In the case of inactive mutation of p53, p53 protein levels did not reflect the p53-driven gene expression. It is expectable that there would be no correlation between p53 and p21 in 15 tumors harboring nonfunctional p53 (Figure 6d, right). However, the p53 level did not correlate with the p21 level even in tumors with functional p53, suggesting that the p53-driven p21 expression was mainly

determined by epigenetic regulation, rather than by the amount of p53 protein. Indeed, PHF2 showed a significant correlation ($r = 0.697$) with p21 in 15 tumors with functional p53 (Figure 6d, left). This result supports our notion that PHF2 is a *bona fide* regulator of p53-driven p21 expression in colon cancer. To confirm this possibility, we analyzed the levels of PHF2, p53 and p21 in colon cancer tissue arrays containing normal and cancer tissue specimens from patients. The demographics of patients are summarized in Supplementary Table 3. In the tissue arrays, PHF2 and p21 levels correlated very well, whereas p53 and p21 levels were not correlated in colon tissues (Figure 6e) and stomach tissues (Figure 6f). Because p53 is often deleted or inactivated in cancers, immunological analyses does not reflect the functionality of p53, which explains the poor correlation between p53 and p21. These results encouraged us to review previous microarray data on *PHF2* mRNA expressions in human colon cancers. Searches of the Cancer Genome Atlas-Colon Adenocarcinoma Gene Expression Data (Data link: http://tcga-data.nci.nih.gov/tcga/) in Oncomine database also revealed that PHF2 is downregulated in colon cancers as compared with normal colon tissues (Figure 6g) and also in stomach cancer gene expression data in the Cancer Genome Atlas (Figure 6h). These findings suggest that PHF2 downregulation contributes to p53 inactivation that occurs during cancer evolution.

DISCUSSION

In the present study, we found that PHF2 is significantly downregulated in colon and stomach cancers and PHF2 suppression is positively associated with p21 suppression in cancers expressing functional p53. Informatics analyses using public databases also demonstrated that PHF2 expression is repressed in colon and stomach cancers. In a tumor xenograft model, PHF2 was found to promote p53-mediated apoptosis induced by anticancer drugs. In response to genotoxic stress, PHF2 was recruited by p53 to the p53 target sites, and facilitated the p53-driven gene expression by demethylating H3K9 in p53 target genes. On the basis of these findings, we propose that PHF2 acts as a tumor suppressor in cancer and enhances p53-mediated DNA damage response in chemotherapy.

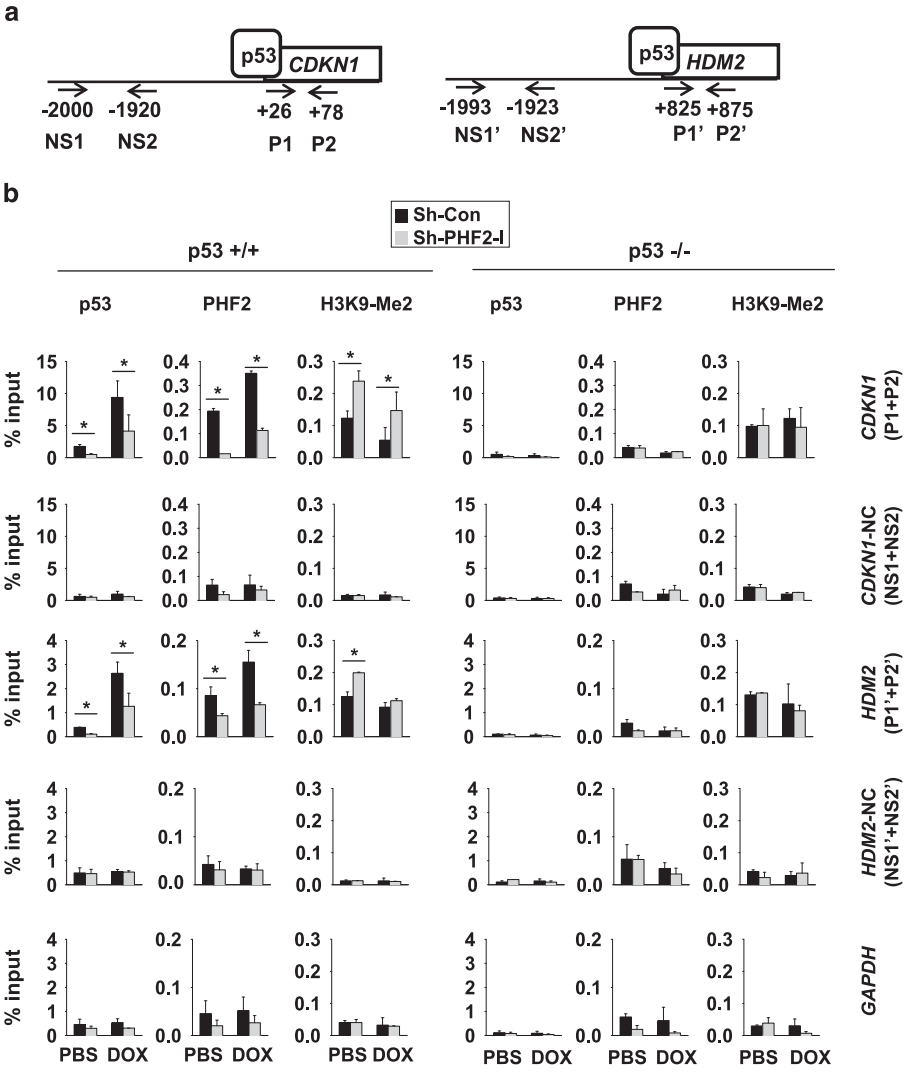

Figure 4. PHF2 acted as an epigenetic coactivator of p53. (**a**) Primer positions for ChIP-qPCR are illustrated. (**b**) p53+/+ and p53 − / − HCT116 and (**c**) HepG2 stably express Sh-Con or Sh-PHF2 RNA cells were treated with 0.5 μM doxorubicin for 16 h, and then cross-linked cell lysates were subjected to ChIP using antibodies against PHF2, p53 or H3K9-Me2. Immunoprecipitated DNAs were analyzed by qPCR using primers specific for the p53 binding elements and negative control sequences in the promoters of *CDKN1A* or *HDM2,* and non-p53 binding *GAPDH* gene promoter as indicated. Bars represent means ± s.d. ($n = 3$) and $^*P < 0.05$ between two groups. (**d**) Schematic figure describing the role of PHF2 in p53 transcriptional activation.

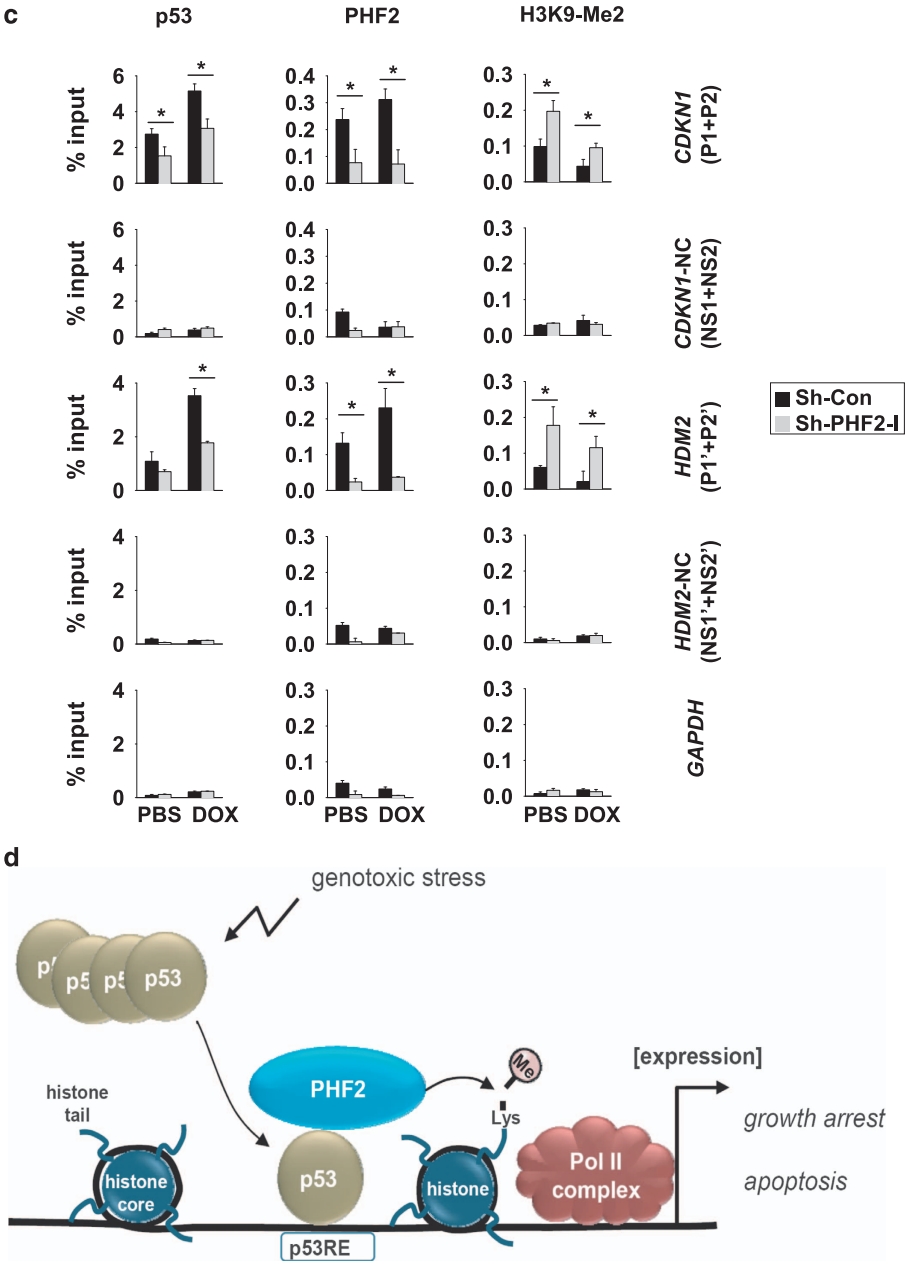

Figure 4. Continued.

Posttranslational modifications of histone tails modulate gene expression by inducing changes in the chromatin structure, and in general, histone acetylation induces gene expression by opening the chromatin for transcription.[17] On the other hand, histone methylation reciprocally regulates gene expression, and its outcome depends on the methylation site, that is, the methylation of H3K9, H3K27 or H4K20 represses transcription, whereas the methylation of H3K4, H3K36 or H3K79 activates transcription.[18,19] In practice, the methylation states of H3K9 and H3K4 are commonly assessed as the markers of the transcriptional activity of promoters, and many reports have concluded that histone modifications are important for the p53 signaling pathway. When cells are under stress, many histone modifying enzymes are recruited to p53 target promoters, and histone methyltransferases, such as G9a and SUV39H1, are downregulated during genotoxic stress, which reduces H3K9 methylation and subsequently enhances p53-driven transcription.[20] Therefore, H3K9 methylation is regarded as a critical step in the control of p53 activity, and thus, H3K9 demethylation might promote the activation of p53. Accordingly, we suggest that H3K9 demethylation by PHF2 functionally activates p53.

The KDM7 family belongs to the Jumonji C superfamily. In humans, the KDM7 family consists of three members, namely, KDM7A (KIAA1718), KDM7B (PHF8) and KDM7C (PHF2).[13] Structurally, the N-terminal halves of KDM7 members contain the JmjC-domain and PHD, and these two domains work cooperatively to demethylate histones, that is, PHD interacts with methylated lysine residues and JmjC-domain removes methyl groups from the lysine residues.[21] In contrast, in BLAST search of NCBI, the C-terminal halves show little homology among the family members and do not contain any known domains. Nonetheless, C-terminal parts of members are essential for their gene regulatory functions, for example, it was found that PHF8 binds to RNA polymerase I/II, KMT2, HCF1, E2F1, ZNF711 and RAR, under

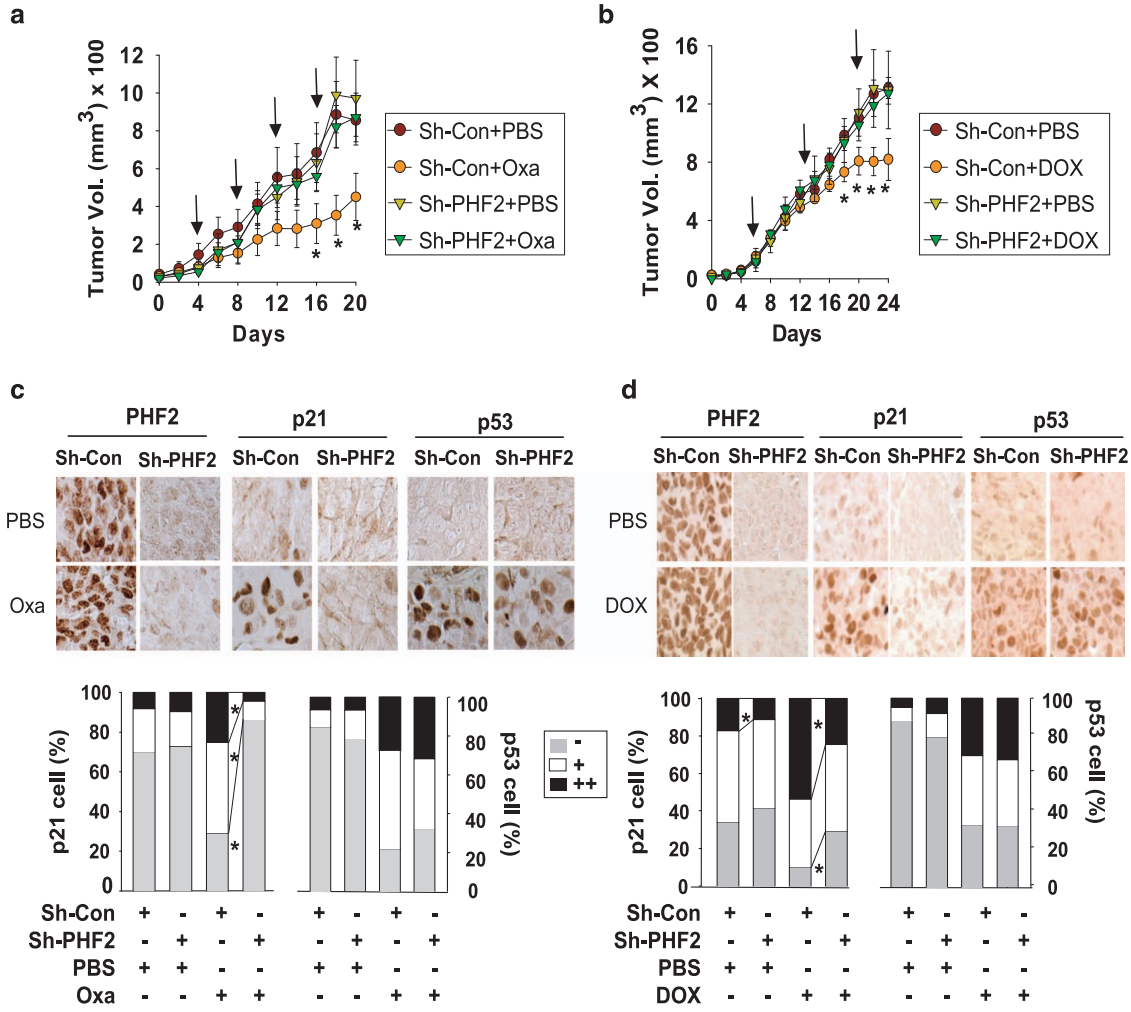

Figure 5. PHF2 was required for the action of anticancer drugs in the xenografts. HCT116 cells, which were infected with Sh-control (Sh-Con) or Sh-PHF2 lentivirus, were implanted in the flanks of nude mice and tumor volumes were measured on alternate days. After Sh-Control or Sh-PHF2 HCT116 tumors had grown to 100–150 mm^3, tumor-bearing mice were intraperitoneally injected with 5 mg/kg of (**a**) oxaliplatin or (**b**) doxorubicin. Arrows indicate the injection time points. Results are presented as means ± s.e. ($n = 10$ for oxaliplatin, $n = 15$ for doxorubicin) and $^*P < 0.05$ versus the Sh-Con group. (**c**, **d**) PHF2, p53 and p21 proteins were immunostained in paraffin-fixed xenografted tumors from mice treated with oxaliplatin (**c**) or doxorubicin (**d**). Pictures were taken under a microscope at ×400 (top). Cells immunopositive for p21 or p53 were counted in three different fields per slide (bottom). Staining levels −, + and ++ were designated as negative, weakly positive or strongly positive, respectively. $^*P < 0.05$ versus the Sh-Con group.

the control of the C-terminal portion of PHF8.[22–25] Likewise, we also found that PHF2 is associated with p53 through its C-terminal region. We surmise that the variability of the C-terminal halves of KDM7 members provides functional diversity by choosing different histone demethylase partners for transcription. Although the structures and biochemical properties of KDM7 members have been identified, the physiological functions of these proteins are not well known. Given that the KDM7 members can remove the methylation from H3K9, H3K27, or H4K20, which is responsible for transcriptional repression they are believed to act as transcriptional coactivators that induce a permissive chromatin state at promoters. This suggests that the functions of KDM7 members might be dependent on the transcription factors that recruit them to the promoters. Recently, it was suggested that PHF2 is involved in energy homeostasis by epigenetically activating HNF4 and FXR,[14] and PHF2 potentiates adipogenesis by acting as a coactivator of CEBPα.[15] Another research group found that PHF2 positively regulated the inflammatory response by epigenetically enhancing the NF-κB-mediated expression of proinflammatory genes.[16] In the present study, it was found that PHF2 interacts with p53 and enhances p53-driven transcription by demethylating H3K9-Me2 at p53 target sites. Actually, the role of PHF2 has not been investigated in detail and its physiological functions are largely unknown. Nevertheless, the above reports and our results indicate that PHF2 participates in diverse physiological responses. More importantly, the present study is the first study to propose a mechanism by which PHF2 has a tumor suppressor role.

p53 is also regulated by direct methylation of its lysine residues. The transcriptional activation of p53 is induced by methylation of its K372 residue by SET7/9.[26] In contrast, p53 methylation at K382 (by SET8) or at K370 (by SMYD2) inhibits its transcriptional activity.[27,28] Initially, we assumed that PHF2 regulates p53 activity by demethylating some lysine residue(s), but this possibility was ruled out because PHF2 interacted with p53 via its C terminus rather than via its N-terminal catalytic domain. When we assessed p53 methylation using an antibody against methylated lysine, levels of methylated p53 were altered minimally by PHF2 knockdown (data not shown). Nonetheless, the possibility that PHF2 demethylates p53 methylation cannot be excluded because we did not assess p53 methylation at specific lysine residues.

Because the *TP53* gene is deleted in many colon cancers, p53 may be a good biomarker for predicting the patient outcome.[29] However, when the *TP53* gene is mutated nonfunctionally in cancer, mutated p53 tends to be highly expressed due to loss of negative feedback regulation, and thus, prognosis cannot be predicted by simply checking the p53 levels.[30] Furthermore, functional p53 is expressed in around half of the colon cancers, although p53 activity is usually repressed. For these reasons, other markers of the p53 signaling pathway are required for predicting the prognosis. p21 lies downstream of p53, and could be a suitable surrogate marker of p53 activity. Indeed, p21, than p53 *per se*, has been shown to be better related to survival among cancer patients.[31,32] In the present study, we checked p21 levels in colon cancer tissues to evaluate p53 activity, and found that p21

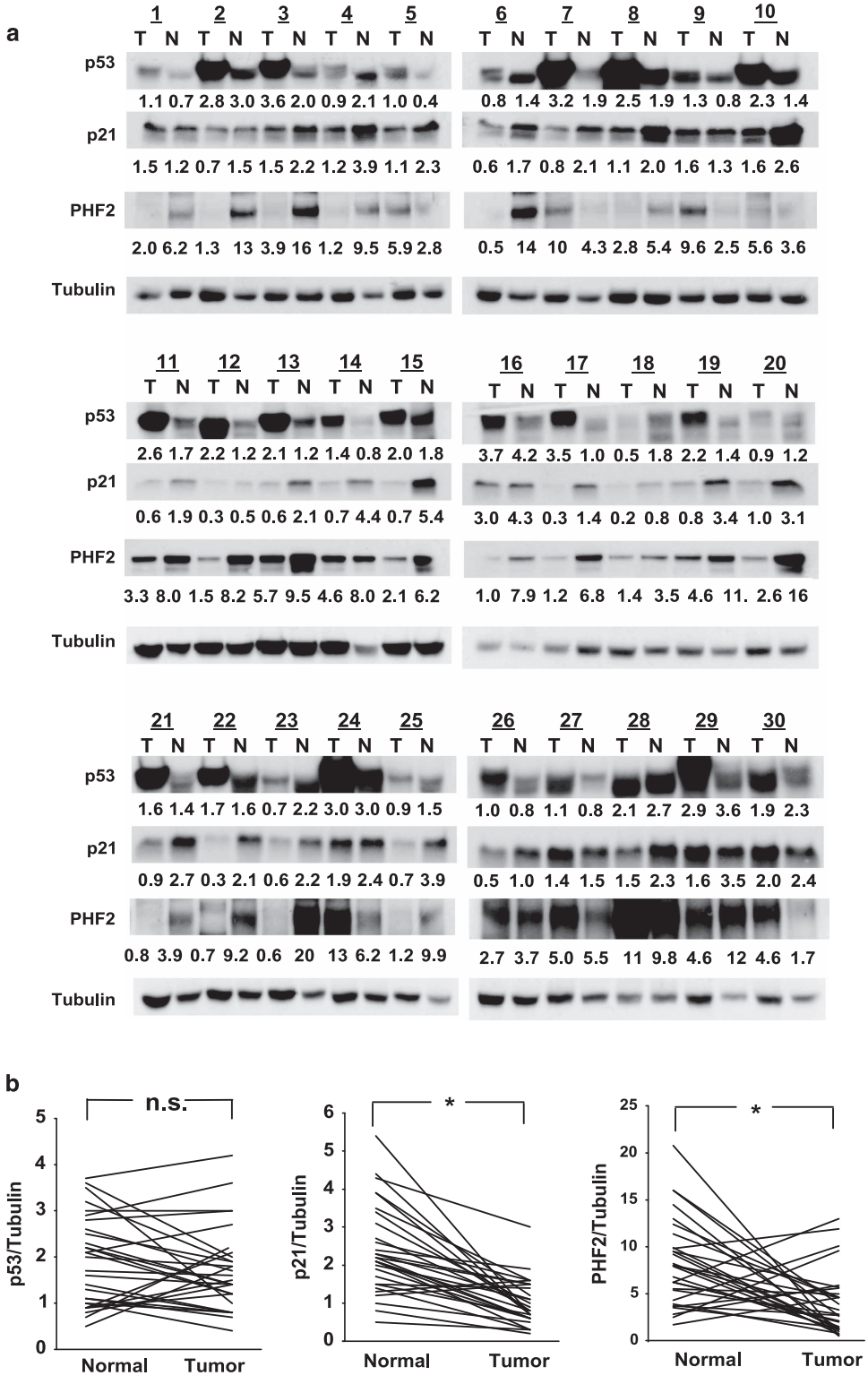

Figure 6. For caption see next page.

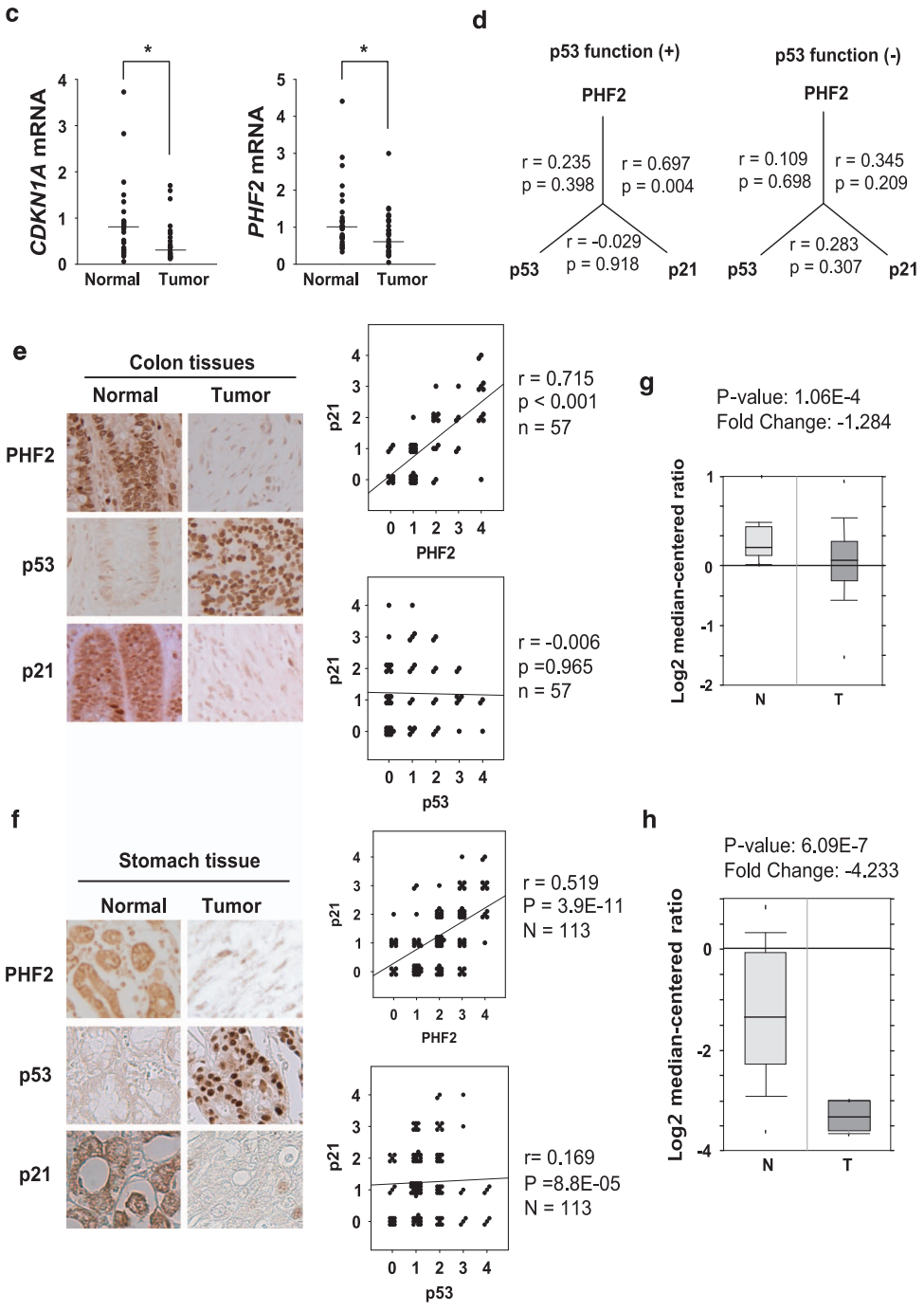

Figure 6. PHF2 was downregulated in colon cancer. (**a**) Malignant tumor (T) and adjacent normal (N) colon tissues were subjected to western blotting using indicated antibodies. Protein bands were densitometrically analyzed and protein levels were normalized to tubulin levels. The relative intensities are presented below each lane. (**b**) Ratios of PHF2, p53 and p21 to tubulin in the tumor and normal tissues of the same patient were plotted individually as a line. *$P < 0.05$ by paired Student's *t*-test. (**c**) mRNAs were extracted from the tumor and normal colon tissues of thirty patients, and *CDKN1A* and *PHF2* mRNA levels were analyzed by RT–qPCR using 18S ribosomal RNA as an internal control. Relative mRNA levels in cancer and normal tissues are indicated by the dotted line, and mean values in tumor and normal tissues are presented as short horizontal bars. *$P < 0.05$ by the paired Student's *t*-test. (**d**) Based on genomic DNA sequencing results and the online database about p53 mutant activities (http://p53.free.fr/), thirty colon tumors were classified as either p53-positive (15 cases) or p53-negative (15 cases). Detailed p53 sequences are provided in Supplementary Table 2. Correlations were determined using Pearson's correlation test. '*r*' and '*p*' represent Pearson's correlation coefficient and *P*-value, respectively. (**e**, **f**) PHF2, p53 and p21 expressions were immunohistochemically evaluated in colon and stomach tissue arrays. All arrays were stained with 3,3′-diaminobenzidine in the same manner and the representative findings are shown (left). Immunoreactivity was evaluated by four reviewers and scored from 0 to 4+. PHF2 versus p21 (right top) and p53 versus p21 (right bottom) levels were individually plotted; points in the same clusters indicate similar expression levels. Correlations were determined using Pearson's correlation test. '*r*', '*p*' and '*n*' represent Pearson's correlation coefficient, *P*-value, and sample number, respectively. (**g**) PHF2 expressions in normal and colon cancer tissues are presented as box plots based on data obtained from the Oncomine database. N, normal colon ($n = 19$); T, colon adenocarcinoma ($n = 101$). (**h**) PHF2 expressions in normal and stomach cancer tissues are presented as box plots based on data obtained from the Oncomine database. N, normal gastric mucosa ($n = 31$); T, gastric adenocarcinoma ($n = 4$). *P*-values (Student's *t*-test) and fold changes were calculated using online programs provided by Oncomine.

expression was not correlated with p53 expression in p53-deleted or p53-mutated colon cancers. Furthermore, somewhat surprisingly, p21 levels were not correlated with p53 levels even in cancer tissues with functional p53. This unexpected finding encouraged us to hypothesize that another critical cofactor has an influence on p53 activity, and here, we conclude that this cofactor is PHF2. In addition, if p53, p21 and PHF2 protein levels are determined in cancer tissues, these triple biomarkers could provide reliable information on p53 function. Particularly, in tumors expressing functional p53, determining the expression levels of PHF2 and p21 could help in predicting patient outcome and tumor response to chemotherapy.

MATERIALS AND METHODS

Materials

Dulbecco's Modified Eagle's medium cell culture media, trypsin, antibiotics, Trizol and Lipofectamine 2000 were purchased from Invitrogen (Carlsbad, CA, USA), MultiScribe Reverse Transcription kit from Applied Biosystems (Carlsbad, CA, USA), and EvaGreen qPCR Mastermix from Applied Biological Materials Inc. (Richmond, British Columbia, Canada). Fetal bovine serum and culture media were obtained from Hyclone Laboratories Inc. (South Logan, UT, USA). Antibodies against p53 (DO-1), p21 and β-tubulin were purchased from Santa Cruz Biotechnology (Santa Cruz, CA, USA), and antibodies against PHF2, Hdm2, H3K4me2, K3K9me2 and Bax were purchased from Cell Signaling (Danvers, MA, USA). Protein A/G-Sepharose beads and Streptavidin Sepharose High Performance beads were purchased from GE Healthcare (Amersham, England), and the luciferase assay kit from Promega (Fitchburg, WI, USA). Oxaliplatin was purchased from Aventis Pharma (Dagenham, UK) and 5-fluorouracil was purchased from Joongwea Pharmaceutical (Seoul, Korea). Doxorubicin and other chemicals were purchased from Sigma-Aldrich (St Louis, MO, USA).

Cell lines, plasmids and transfection

The HEK293T human embryonic kidney cell line was purchased from American Type Culture Collection (Rockville, MD, USA). HCT116 (p53+/+ and p53−/−) human colon cancer cell lines were kindly donated by Professor Deug Y Shin (Dankook University, Korea). All other cell lines were purchased from Korean Cell Line Bank (Seoul, Korea). The cell lines were passaged for fewer than six months after being authenticated by DNA fingerprinting, which was performed using AmplFLSTR identifiler PCR Amplification kit (Applied Biosystems, CA, USA) by Korean Cell Line Bank. The cell lines were cultured in Dulbecco's Modified Eagle's medium or RPMI1640 supplemented with 10% fetal bovine serum at 37 °C in 5% CO_2. Full-length p53 and PHF2 cDNAs were cloned by RT–PCR with specific primers (Supplementary Table 1), and amplified using a *Pfu* DNA polymerase. p53 and PHF2 cDNAs were inserted into the hemagglutinin (HA)- or Flag/Streptavidin binding protein (F/S)-tagged vectors, respectively. Mutated p53 and PHF2 plasmids were constructed from the HA-p53 and F/S-PHF2 by PCR (Supplementary Table 1) and recloned using EcoRI and BamHI restriction enzymes. Plasmids were transfected into the cells using Lipofectamine 2000, and cells were collected 36–48 h after transfection. For gene silencing, the pLKO.1-puro vector was purchased from Sigma-Aldrich and oligonucleotides targeting the green fluorescent protein (control shRNA) or PHF2 were inserted into the vector using AgeI and EcoRI restriction enzymes. The viral vector was co-transfected with pMD2-VSVG, pRSV-RRE and pMDLg/pRRE helper DNA into HEK293T cells, and the viral supernatant was collected. HCT116 cells were infected overnight with the virus in the presence of 6 μg/ml of polybrene. After selecting infected cells using puromycin (2 μg/ml), gene silencing was confirmed by western blotting and RT–qPCR.

In vivo xenograft mouse model

HCT116 colon tumors were grafted into nude mice (SLC Inc., Shizuoka, Japan), as previously described.[33] Briefly, sh-control or Sh-PHF2 HCT116 p53+/+ stable cells (5×10^6) were injected subcutaneously into the flanks of five mice. After tumor volumes had reached 100–150 mm^3, tumor-bearing mice were injected intraperitoneally with oxaliplatin (5 mg/kg) twice a week or doxorubicin (5 mg/kg) weekly along with the injection of phosphate-buffered saline in the control group; tumor sizes were measured every other day. The day after the last injection, tumors were excised from the mice under 30 mg/kg Zoletil and 10 mg/kg Xylazine anesthesia. Data were collected from three independent experiments. The procedures performed and the care of animals were in accordance with the guidelines of the Seoul National University Laboratory Animal Maintenance Manual (permission # SNU-110531-1).

Human colon cancer tissues and tissue arrays

Thirty colon cancer tissues and their matched adjacent normal tissues were obtained from the tissue bank of Seoul National Hospital after the Institutional Review Board permission (C-1202-039-397). Detailed information of each sample is provided in Supplementary Table 2. Tissue arrays containing colon cancer, stomach cancer and normal tissues were obtained from SuperBioChips (Seoul, Korea). Patient's demographic information is available online (www.tissue-array.com). CDA3 chip was used for testing colon cancer and normal tissues. CQ2 and CQN2 chips were used for stomach cancer and normal tissues, respectively.

Cell cycle and viability analyses

To analyze the cell cycle, cells were collected after the experiments and fixed with 70% ethanol at −20 °C for 16 h. After washing three times with phosphate-buffered saline, cells were incubated with 10 μg/ml of propidium iodide and 100 μg/ml of RNase at 37 °C for 30 min, and their DNA contents were analyzed using a fluorescence-activated cell sorter (FACS). To check cell viability, cells were incubated with 0.5 mg/ml of MTT (3-(4,5-dimethylthiazol-2-yl)-2,5-diphenyltetrazolium bromide) for 2 h at 37 °C. The precipitated purple formazan was solubilized with dimethyl sulfoxide, and quantified at 570 nm by spectrophotometry.

RNA isolation and RT–qPCR

Total RNA was extracted using Trizol according to the manufacturer's instructions (Ambion, Austin, TX, USA). For each reverse transcription, 1 μg of total RNA was used for cDNA synthesis using a MultiScribe Reverse Transcription kit. *PHF2, CDKN1A, HDM2* and *BAX* mRNAs were analyzed by using an EvaGreen qPCR Mastermix with StepOne Real-Time PCR System (Applied Biosystems). 18S ribosomal RNA was used as an internal control. PCR primer sequences are listed in Supplementary Table 1.

Western blotting

Frozen tissues were pulverized in a mortar and lysed in RIPA buffer (150 mM NaCl, 50 mM Tris-HCl (pH 7.2), 0.5% NP-40, 1% Triton X-100, 1% sodium deoxycholate) containing a protease inhibitor cocktail. Tissue lysates were separated on 8–10% SDS-polyacrylamide gels and transferred to an Immobilon-P membrane. Membranes were blocked with 5% nonfat milk in TBS-T for 1 h, and then incubated overnight at 4 °C with a primary antibody diluted 1:1000. Membranes were incubated with a horseradish peroxidase–conjugated secondary antibody (1:5000) for 1 h, and developed using the ECL-plus kit (Thermo Scientific, Rockford, IL, USA). Proteins were analyzed using antibodies against the indicated antigens.

Immunoprecipitation and pull-down analysis

For immunoprecipitation, cell lysates (1 mg of protein) were incubated with 5 μl of a primary antibody at 4 °C for 16 h, and then with 10 μl of protein A/G-Sepharose beads for 2 h at 4 °C. Bead-bound proteins were eluted with SDS sample buffer and then subjected to SDS–polyacrylamide gel electrophoresis and western blotting. For streptavidin-binding peptide pull-down analysis, cell lysates (1 mg of protein) were applied to Streptavidin Sepharose High Performance beads overnight at 4 °C. Bead-bound proteins were eluted with biotin and then subjected to SDS-polyacrylamide gel electrophoresis and western blotting.

Chromatin immunoprecipitation

A total of 5×10^6 cells were cross-linked with 1% formaldehyde for 10 min at room temperature, and then glycine (final concentration 125 mM) was added to quench the cross-linking reaction. Chromatin complexes were sonicated and then precipitated with the indicated antibodies overnight at 4 °C. Precipitated DNAs were purified, amplified and quantified using the ABI StepOne Real-Time PCR System and EvaGreen qPCR Mastermix. PCR primer sequences used for ChIP are listed in Supplementary Table 1.

Immunohistochemistry

Immunohistochemical analyses of xenografted tumors and human tissues were performed, as previously described.[33] Histology and immunostaining were reviewed under a microscope at a ×400 magnification, and the images were captured using Leica DM2500 camera and Leica Application Suite Ver. 3.8.0 software (Leica, Wetzlar, Germany). The expressions of p21, p53 and PHF2 were quantified by counting the number of immunopositive cells per square millimeter in each image. All slides were reviewed independently by four experts, and the results obtained were classified into five grades.

Informatics data analysis

The informatics data on *PHF2* mRNA expression in colon and stomach cancers were obtained from two independent studies in the Oncomine database.[34] The standardized normalization techniques and statistical calculations for the normal versus cancer analysis are described in the Oncomine web site (www.oncomine.com). Initially, microarray raw data were analyzed by a standard method using either the Robust Multichip Average for Affymetrix data or the Loess Normalization for cDNA array data. To scale down the data and allow comparisons with independent studies, *Z*-score normalization was applied, which included log2 transformation, and setting the median of the array to 0 and the standard deviation of the array to 1.

Statistical analyses

All data were analyzed using the Microsoft Excel 2007 software, unless otherwise stated. Continuous variables were analyzed using Student's *t*-test when the data were normally distributed. The statistical methods used for non-normally distributed data are described in 'Figure legends'. Pearson's correlation test (IBM SPSS Statistics 19, Chicago, IL, USA) was used for the correlation analysis. All statistical tests were two-sided, and significance was accepted at P-values < 0.05.

CONFLICT OF INTEREST

The authors declare no conflict of interest.

ACKNOWLEDGEMENTS

This work was supported by a Korean Health Technology R&D grant (A121106, A120476), National Research Foundation grants of Korea (2009-0066985, 2011-0008634 and 2011-0030737) and by a grant from the Seoul National University Hospital Research Fund 2011 (0320110180).

REFERENCES

1 Levine AJ, Oren M. The first 30 years of p53: growing ever more complex. *Nat Rev Cancer* 2009; **9**: 749–758.
2 Riley T, Sontag E, Chen P, Levine A. Transcriptional control of human p53-regulated genes. *Nat Rev Mol Cell Biol* 2008; **9**: 402–412.
3 Murray-Zmijewski F, Slee EA, Lu X. A complex barcode underlies the heterogeneous response of p53 to stress. *Nat Rev Mol Cell Biol* 2008; **9**: 702–712.
4 Gu W, Shi X-L, Roeder RG. Synergistic activation of transcription by CBP and p53. *Nature* 1997; **387**: 819–823.
5 Gu W, Roeder RG. Activation of p53 sequence-specific dna binding by acetylation of the p53 C-terminal domain. *Cell* 1997; **90**: 595–606.
6 Sakaguchi K, Herrera JE, Si Saito, Miki T, Bustin M, Vassilev A *et al.* DNA damage activates p53 through a phosphorylation–acetylation cascade. *Genes Dev* 1998; **12**: 2831–2841.
7 Legube G, Linares LK, Tyteca S, Caron C, Scheffner M, Chevillard-Briet M *et al.* Role of the Histone Acetyl Transferase Tip60 in the p53 Pathway. *J Biol Chem* 2004; **279**: 44825–44833.
8 Jin L, Hanigan CL, Wu Y, Wang W, Park BH, Woster PM *et al.* Loss of LSD1 (lysine-specific demethylase 1) suppresses growth and alters gene expression of human colon cancer cells in a p53- and DNMT1(DNA methyltransferase 1)-independent manner. *Biochem J* 2013; **449**: 459–468.
9 Wiesner GL, Daley D, Lewis S, Ticknor C, Platzer P, Lutterbaugh J *et al.* A subset of familial colorectal neoplasia kindreds linked to chromosome 9q22.2-31.2. *Proc Natl Acad Sci* 2003; **100**: 12961–12965.
10 Sinha S, Singh R, Alam N, Roy A, Roychoudhury S, Panda C. Alterations in candidate genes PHF2, FANCC, PTCH1 and XPA at chromosomal 9q22.3 region: Pathological significance in early- and late-onset breast carcinoma. *Mol Cancer* 2008; **7**: 84.
11 Ghosh A, Ghosh S, Maiti GP, Mukherjee S, Mukherjee N, Chakraborty J *et al.* Association of FANCC and PTCH1 with the development of early dysplastic lesions of the head and neck. *Ann Surg Oncol* 2012; **19**: 528–538.
12 Hasenpusch-Theil K, Chadwick BP, Theil T, Heath SK, Wilkinson DG, Frischauf A-M. PHF2 a novel PHD finger gene located on human Chromosome 9q22. *Mamm Genome* 1999; **10**: 294–298.
13 Wen H, Li J, Song T, Lu M, Kan P-Y, Lee MG *et al.* Recognition of histone H3K4 trimethylation by the plant homeodomain of PHF2 modulates histone demethylation. *J Biol Chem* 2010; **285**: 9322–9326.
14 Baba A, Ohtake F, Okuno Y, Yokota K, Okada M, Imai Y *et al.* PKA-dependent regulation of the histone lysine demethylase complex PHF2-ARID5B. *Nat Cell Biol* 2011; **13**: 668–675.
15 Okuno Y, Ohtake F, Igarashi K, Kanno J, Matsumoto T, Takada I *et al.* Epigenetic regulation of adipogenesis by PHF2 histone demethylase. *Diabetes* 2012; **33**: 1426–1434.
16 Stender Joshua D, Pascual G, Liu W, Kaikkonen Minna U, Do K, Spann Nathanael J *et al.* Control of proinflammatory gene programs by regulated trimethylation and demethylation of histone H4K20. *Mol Cell* 2012; **48**: 28–38.
17 Kurdistani SK, Grunstein M. Histone acetylation and deacetylation in yeast. *Nat Rev Mol Cell Biol* 2003; **4**: 276–284.
18 Jaskelioff M, Peterson CL. Chromatin and transcription: histones continue to make their marks. *Nat Cell Biol* 2003; **5**: 395–399.
19 Schneider R, Grosschedl R. Dynamics and interplay of nuclear architecture, genome organization, and gene expression. *Genes Dev* 2007; **21**: 3027–3043.
20 Mungamuri SK, Benson EK, Wang S, Gu W, Lee SW, Aaronson SA. p53-mediated heterochromatin reorganization regulates its cell fate decisions. *Nat Struct Mol Biol* 2012; **19**: 478–484.
21 Fortschegger K, Shiekhattar R. Plant homeodomain fingers form a helping hand for transcription. *Epigenetics* 2011; **6**: 4–8.
22 Feng W, Yonezawa M, Ye J, Jenuwein T, Grummt I. PHF8 activates transcription of rRNA genes through H3K4me3 binding and H3K9me1/2 demethylation. *Nat Struct Mol Biol* 2010; **17**: 445–450.
23 Kleine-Kohlbrecher D, Christensen J, Vandamme J, Abarrategui I, Bak M, Tommerup N *et al.* A functional link between the histone demethylase PHF8 and the transcription factor ZNF711 in X-linked mental retardation. *Mol Cell* 2010; **38**: 165–178.
24 Qiu J, Shi G, Jia Y, Li J, Wu M, Dong S *et al.* The X-linked mental retardation gene PHF8 is a histone demethylase involved in neuronal differentiation. *Cell Res* 2010; **20**: 908–918.
25 Liu W, Tanasa B, Tyurina OV, Zhou TY, Gassmann R, Liu WT *et al.* PHF8 mediates histone H4 lysine 20 demethylation events involved in cell cycle progression. *Nature* 2010; **466**: 508–512.
26 Chuikov S, Kurash JK, Wilson JR, Xiao B, Justin N, Ivanov GS *et al.* Regulation of p53 activity through lysine methylation. *Nature* 2004; **432**: 353–360.
27 Huang J, Perez-Burgos L, Placek BJ, Sengupta R, Richter M, Dorsey JA *et al.* Repression of p53 activity by Smyd2-mediated methylation. *Nature* 2006; **444**: 629–632.
28 Shi X, Kachirskaia I, Yamaguchi H, West LE, Wen H, Wang EW *et al.* Modulation of p53 Function by SET8-Mediated Methylation at Lysine 382. *Mol Cell* 2007; **27**: 636–646.
29 Munro AJ, Lain S, Lane DP. P53 abnormalities and outcomes in colorectal cancer: a systematic review. *Br J Cancer* 2005; **92**: 434–444.
30 Brosh R, Rotter V. When mutants gain new powers: news from the mutant p53 field. *Nat Rev Cancer* 2009; **9**: 701–713.
31 Zirbes TK, Baldus SE, Moenig SP, Nolden S, Kunze D, Shafizadeh ST *et al.* Prognostic impact of p21/waf1/cip1 in colorectal cancer. *Int J Cancer* 2000; **89**: 14–18.
32 Ogino S, Nosho K, Shima K, Baba Y, Irahara N, Kirkner GJ *et al.* p21 Expression in Colon Cancer and Modifying Effects of Patient Age and Body Mass Index on Prognosis. *Cancer Epidemiol Biomarkers Prev* 2009; **18**: 2513–2521.
33 Yeo E-J, Chun Y-S, Cho Y-S, Kim J, Lee J-C, Kim M-S *et al.* YC-1: A Potential Anticancer Drug Targeting Hypoxia-Inducible Factor 1. *J Natl Cancer Ins* 2003; **95**: 516–525.
34 Skrzypczak M, Goryca K, Rubel T, Paziewska A, Mikula M, Jarosz D *et al.* Modeling Oncogenic Signaling in Colon Tumors by Multidirectional Analyses of Microarray Data Directed for Maximization of Analytical Reliability. *PLoS ONE* 2010; **5**: e13091.

Supplementary Information accompanies this paper on the Oncogene website (http://www.nature.com/onc)